Deformation of the compound middle lamella in spruce latewood by micro-pillar compression of double cell walls

Rejin Raghavan · Ramesh-Babu Adusumalli ·
Gerhard Buerki · Silla Hansen · Tanja Zimmermann ·
Johann Michler

Abstract The mechanical integrity of the interface between two adjacent cells in spruce late wood was studied by uniaxial compression of focused ion beam machined micro-pillars of double cell walls (DCW) containing the compound middle lamella (CML). The DCW reveals a lower yield strength and stiffness than the secondary cell wall (S2). Failure occurs by tearing of the interface between the first (S1) and second layers (S2) of the secondary cell wall exposing the internal arrangement of the microfibrils, while the CML remains intact.

Introduction

The wood cell wall, a master piece of evolutionary design has evolved to provide mechanical strength for the living tree. It can be seen as a bio-composite organized in layers with different thicknesses and different portions of the three main chemical components: the polysaccharides cellulose, hemicellulose, and the polyphenolic lignin [1]. Cellulose fibril aggregates are arranged in different angles (microfibril angle, MFA) in the secondary cell wall layers S1, S2, and S3, respectively. In S1 and S3 layers of spruce latewood, microfibrils are oriented almost perpendicular to the fiber axis, whereas in S2 layers microfibrils are oriented almost parallel to the fiber axis [2]. The S2 layer with the highest cellulose concentration is the by far thickest cell wall layer (up to 90 % of the entire cell wall), thus of utmost importance for the strength and stiffness of wood [3]. The S1 layer in late wood of spruce occupies up to 9 % of the entire cell wall, thickness being in the range of 0.38 μm [3]. The cell walls are linked by the compound middle lamella (CML) (primary wall + middle lamella [ML]) with highest concentration of lignin and pectins.

In addition to several conventional mechanical testing, the micro-mechanical behavior of several wood species has been studied using novel ex-situ or in situ SEM custom-made set-ups [4–9]. But, for a better understanding of the mechanical performance of wood, clear understanding of the strength, stiffness, and deformation behavior of single wood fibers and their respective cell wall layers is needed. Some studies have investigated the mechanical properties of single softwood tracheids or hardwood fibers, which were mechanically or chemically isolated from wood [10–14]. Past research also focused on the estimation and measurement of mechanical properties of wood cell wall layers such as hardness and stiffness by means of nanoindentation tests [15–17], where wood is embedded in low viscosity epoxy resin. Direct measurement on cell walls was reported recently in the form of cell wall bending, which was performed using an AFM tip mounted on a micromanipulator [18]. The cell walls were fabricated from a wood slice by using focused ion beam (FIB) machining.

While these nano-scale experiments provide useful insights into the S2 cell wall mechanics, it would be easier to interpret the mechanical response in a simple load case.

R. Raghavan (✉) · G. Buerki · S. Hansen · J. Michler
Laboratory for Mechanics of Materials and Nanostructures,
Swiss Federal Laboratories for Materials Science and
Technology—EMPA, 3602 Thun, Switzerland
e-mail: rejin.koodakal@empa.ch

R.-B. Adusumalli
Department of Chemical Engineering, Birla Institute of
Technology & Science, Pilani, Hyderabad Campus, Hyderabad
500078, Andhra Pradesh, India

T. Zimmermann
Applied Wood Materials, Swiss Federal Laboratories for
Materials Science and Technology—EMPA, 8600 Duebendorf,
Switzerland

Recently, it was demonstrated that the technique of micro-pillar compression, which is used for studying size effects in metals and ceramics, can also be used to study the deformation and failure mechanisms of individual cell walls [19, 20]. Here, micro-pillars comprising only S2 layer, were fabricated out of the wood cell walls of spruce tracheids, using FIB technique. In particular, Adusumalli et al. [19] have shown that the secondary cell wall (S2) exhibits yield strength values of ∼160 MPa and large scale plasticity. Formation of a kink band was also observed during the compression of S2 cell wall micro-pillars. In addition, a model for deformation and failure mechanism of the S2 cell wall has been proposed via cross-sectional analysis of the micro-pillars post compression. The feasibility and reliability of this novel methodology was also demonstrated by studying Keranji (*Dialium* ssp.), a dense Asian hardwood, and Loblolly pine (*Pinus taeda*), an American softwood [20]. These findings and analysis gave rise to the following outstanding questions.

What is the role of the ML in terms of structural integrity? The ML glues the cells together to form the tissue and this layer is in principle free of cellulose. The transition from the ML to the adjacent cell wall layers is not clear; hence the combination of the ML and both adjacent P (primary wall) layers is referred to as the CML, generally known as CML [3]. How does the strength and toughness of the interface between the S1 (thin layer) and CML (thin layer) correspond to that of the S2 (thick layer)? Hence, the objective of this study was to investigate deformation and failure mechanisms of double cell walls (DCWs) consisting of CML, S1, and S2 layers (S2 + S1 + CML + S1 + S2). Cylindrical pillars with diameter of 3 μm were prepared by FIB machining of spruce latewood tracheids. The mechanics and deformation response were studied by in situ SEM compression of the micro-pillars.

Materials and methods

Preparation of double cell wall pillars

Longitudinal specimens of round spruce wood blocks (diameter ∼3 mm; length ∼8 mm) with a moisture content of about 6 % were microtomed across the cell diameter using a Reichert-Jung Polycut E (Germany). Successive sections of 100, 10, and 1 μm thickness were cut from top surface using diamond knife with the speed of 500, 1000, and 2000 rpm, respectively. Smooth surfaces of cell wall cross-sections were achieved after ∼5 min sectioning of 1 μm slices. After microtoming, rectangular blocks were cut out of the round blocks using a razor blade in order to map the latewood cells. Specimens were coated with 10 nm thick gold–palladium to minimize charging and e-beam damage [21]. Twelve cylindrical pillars consisting of CML, S1, and a part of the S2 layer with diameter of 3 μm and aspect ratio of 2–2.5 were FIB machined from the longitudinal-tangential side of the latewood zone using a Tescan Lyra FIB (Brno, Czech Republic) (Fig. 1). The FIB machining was carried out in two steps using a Ga$^+$ beam with energy of 30 and 10 keV. Initially, rough milling was performed with a high Ga$^+$ beam current (3500 pA) to obtain a pillar of ∼8 μm diameter in a crater of ∼40 μm. Next, fine polishing was performed using 10 keV and low Ga$^+$ beam current (80 pA) to minimize beam damage and to obtain the final pillar of 3 μm diameter as shown in Fig. 1c.

Mechanical testing of cell wall pillars

The micro-pillars were compressed in displacement control (strain rate of 10^{-3}/s) using an indigenously built in situ SEM (Zeiss DSM962) nanoindenter. A detailed description of the in situ SEM nanoindenter is available elsewhere
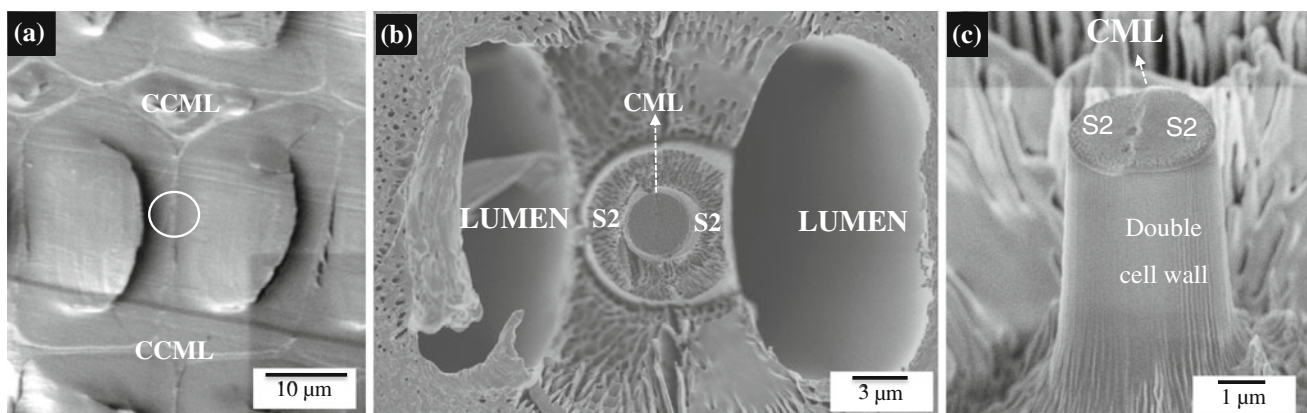

Fig. 1 a Overview showing a typical location (*circle*) used for FIB machining of pillars. **b** Top view of one such DCW pillar. **c** Inclined view (tilt = 50) of the similar pillar revealing orientation of the microfibrils; *S2* secondary wall layer, *CML* compound middle lamella, *CCML* cell corner middle lamella

[22]. A conical flat punch diamond indenter with tip diameter of around 6 µm was used for compression of the micro-pillars. The micro-pillars were imaged a priori and post compression by a cold emission SEM (Hitachi 4800) for studying the cell wall deformation and failure mechanisms. All measurements were carried out in an environment of 10^{-6} mbar and 23 °C.

Results and discussion

The role of the CML in the mechanical response of a wood species is important both from scientific and technological perspectives. While the macro-mechanical behavior of a wood block is studied by considering wood as a cellular foam, the structure and mechanical behavior of the interface between two adjoining tracheids is ignored. The values of the interfacial strength and insights obtained from the mechanical behavior are valuable for the process of papermaking, especially in mechanical pulping.

Deformation

Figure 2 shows the stress–strain response of a DCW micro-pillar in comparison with that of a S2 cell wall [19]. It can be observed that the yield strength (125 ± 20 MPa) and the elastic modulus (E) of the DCW are lower than that of the S2 cell wall. Possible reasons are discussed next.
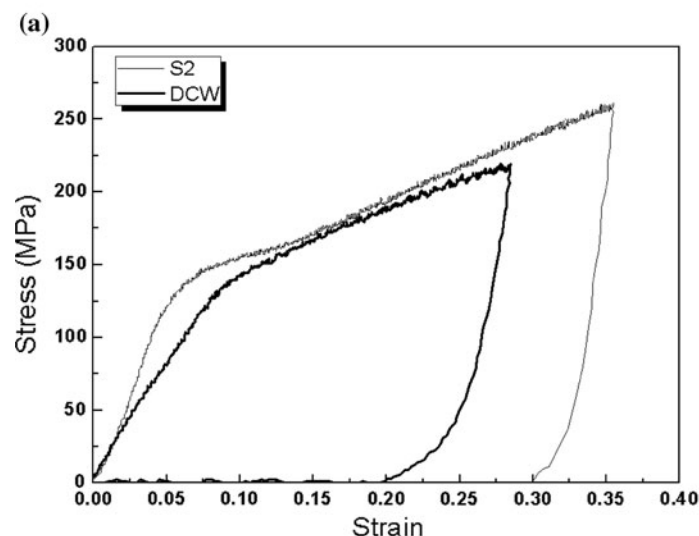
- Nanoindentation of the cell corner middle lamella (CCML) reveals that the hardness (H) and E of CCML are lower than H and E of S2 cell wall because of a high content of lignin (>60 %) and pectin [16].
- Microfibril orientation within the S2 pillar is more or less uniform. But, the same cannot be said about the microfibril orientation of DCW pillar (S2 + S1 + P + ML + P + S1 + S2). In fact, the orientation of the microfibrils especially in P and S1 layers are not clearly defined. In P layer, microfibrils are randomly oriented and in S1 layer, microfibrils are oriented almost perpendicular to the fibers axis but in literature some crossed structures are also reported for S1 layer [2]. Small MFAs (2–5°) like in S2 layer in conjunction with the high stiffness of the cellulose fibers give rise to a large modulus of elasticity, while large angles (70°–90°) like in the S1 or a disordered structure like in the CML layer lead to higher elongation at break. It should be noted that DCW curve shown in Fig. 2a represents the stress–strain curve before fracture. The slight misorientation of the microfibrils in S2 cell wall could be reason for the observed bi-phasic (change in slope after the yield point) behavior in S2 curve (Fig. 2a) [19].

Fracture

Figure 3 shows the stress–strain response of a DCW micro-pillar up to failure in comparison with that of a S2 cell wall.
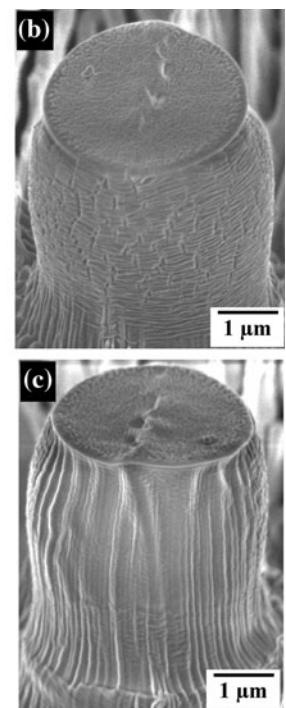

Fig. 2 a A stress–strain curve obtained from compression of *DCW* micro-pillar is compared to that from a *S2* cell wall. **b, c** Post compression HRSEM images of diametrically opposite faces of the DCW micro-pillar

Fig. 3 a A stress–strain curve obtained from compression of *DCW* micro-pillar is compared to that from a *S2* cell wall. **b, c** Post compression HRSEM images of diametrically opposite faces of the DCW micro-pillar showing asymmetric failure regions. The *white arrow* in **b** shows the location of the ML
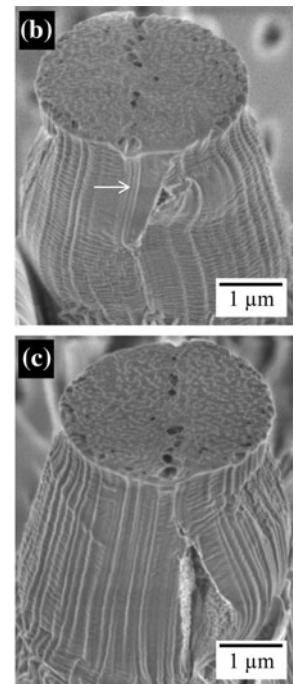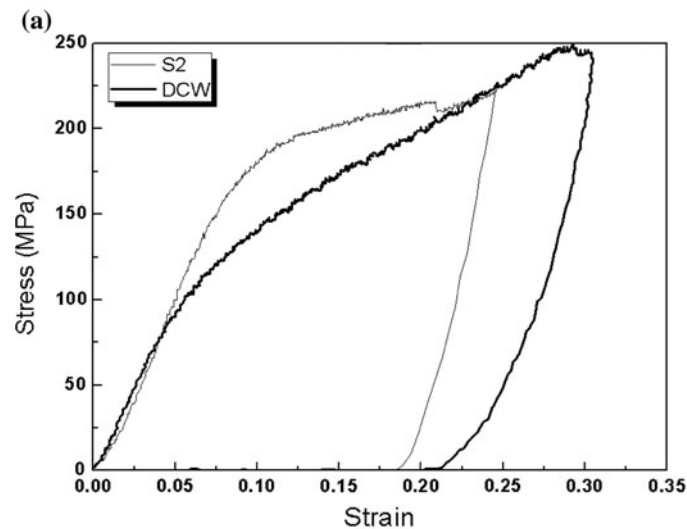
It is interesting to note that the failure of the DCW micro-pillar does not occur along the CML, but along an interface parallel and adjacent to the CML. This observation is in contrast to the failure of the S2 cell wall, which occurs by the formation of a kink with a corresponding stress drop in the stress–strain curve. While abrupt stress drops are not seen in the response of the DCW, a serrated flow behavior is noted. This suggests that failure of the DCW micro-pillar occurs by a tearing mechanism and not sudden crack propagation.

Nevertheless, it is important to note that the absolute values of strength and stiffness, the fracture behavior, and also the fracture path might have been influenced by the ambience and are only valid for the measuring and sample conditions.

Interface anatomy revealed by fracture

The deformation and failure of the cell wall reveals interesting features of wood anatomy, which are difficult to access by conventional structural characterization techniques. In this study, it is observed that the failure of the DCW is not initiated at the CML, but most probably at the interface between S1 and S2, which is supported by earlier studies of abrupt change in MFA orientation at the S1–S2 interface [23, 24]. It also can be supported by the fact that high MFA of S1 layer (70°–90°) is responsible for transverse elastic modulus of spruce latewood [25] and low MFA of S2 layer (0°–10°) is responsible for longitudinal elastic modulus of wood [3]. Figure 4 shows high

resolution scanning electron microscopy (HRSEM) images of the S1–S2 interface, which was torn during micro-compression. It is interesting to note fractured microfibril ligaments protruding from both faces of the separated interface. It is assumed that broken ligaments correspond to S1 layer and thus providing evidence that microfibrils in S1 layer are more or less perpendicular to the fiber axis as described in the literature. It could also be assumed that these broken ligaments appear as fines on agglomeration during mechanical pulping, in which the main aim is to separate the wood cells from the ML by mechanical forces [26]. Figure 5 shows a schematic representation of the proposed failure mechanism found during compression of the DCW micro-pillars. In Fig. 4b, inclined view of DCW after compression, crack can be observed at S1–S2 interface, whereas CML remained as crack-free zone.

It is noteworthy in this context that transmission electron microscopy (TEM) of ultra-thin sections of Norway spruce tracheids showed that the strongly lignified CML also includes the outer part of the S1-layer, i.e., the outer part of the S1-layer may on occasions be strongly lignified [27]. Hence, the bridging microfibrils observed at the S1–S2 interface in this study may come from such an outer part of the S1 layer. In some cases, the microfibrils are intact and form a bridge across the interface, which could be from the outer part of the S2 layer. Crack bridging is found to enhance toughness in a variety of materials and their composites [28]. This is a new and important observation, which suggests that the CML is tougher (more resistance to cracking) than the individual cell walls, as shown in Figs. 2 and 3.
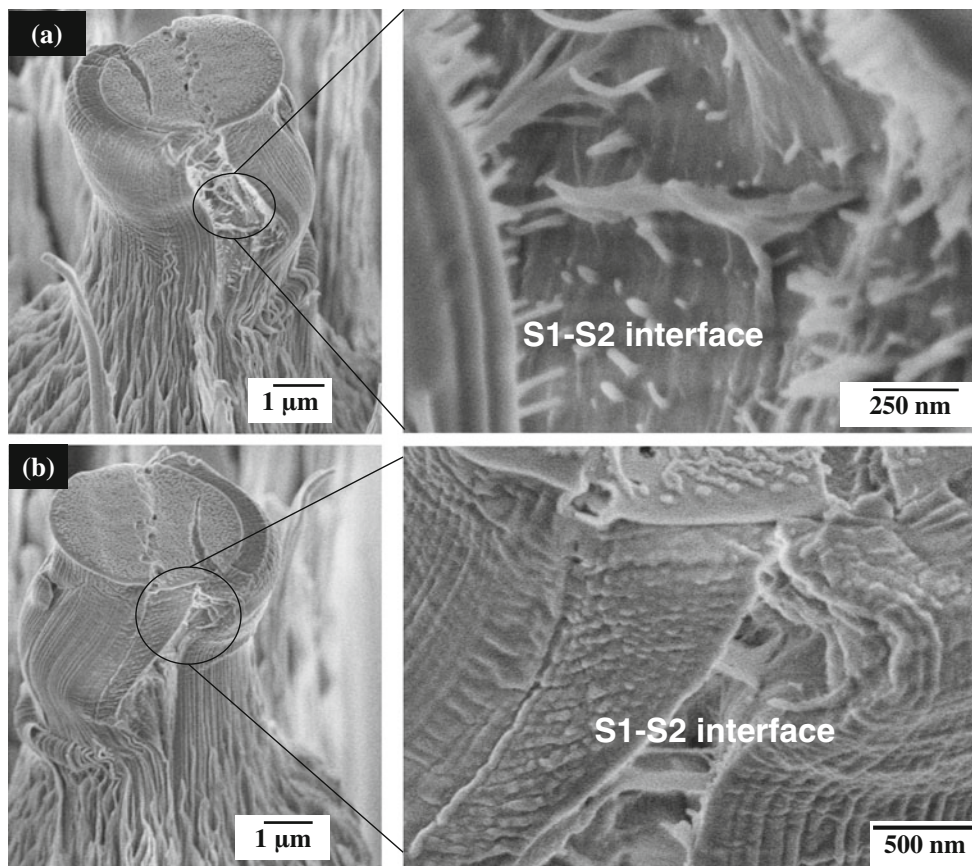
Fig. 4 Post compression HRSEM images highlighting failure features of the *DCW* pillar. **a** Protruding broken ligaments and intact bridging microfibrils are observed at the *S1–S2* interface. **b** Diametrically opposite view of same pillar exhibiting stretched ligaments across the *S1–S2* interface

Fig. 5 Schematic diagram showing the asymmetric nature of the failure at the *S1–S2* interface during *DCW* micro-compression. *S2* and *S1* are secondary cell wall layers in which microfibrils are oriented parallel and perpendicular to the fibers axis, respectively, where as in primary wall (*P*) microfibrils are oriented randomly and *ML* represents the middle lamella
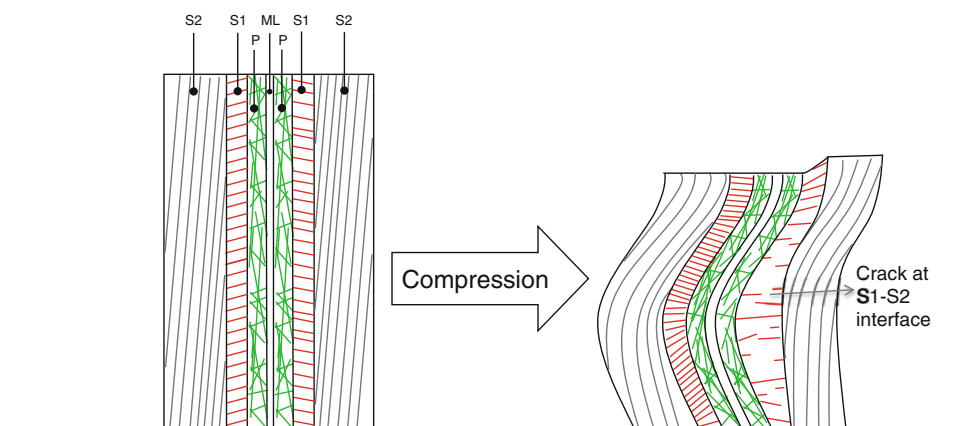
Conclusions

The deformation and failure mechanisms of the CML in spruce wood and its adjacent cell wall layers were studied by compression of FIB machined DCW micro-pillars. While lower strength and stiffness values compared to the secondary cell wall were obtained, the failure was found to occur at the interface between the S1 and S2 layers. The observation of broken ligaments could explain the fines in mechanical pulping that might stem from S1 layers. Similarly, the observation of microfibrils bridging across the separated interface provides valuable insights into the structure and gives explanations for the toughness of the wood.

References

1. Klemm D, Heublein B, Fink HP, Bohn A (2005) Angewandte Chemie Int Ed 44:3358
2. Brandström J (2002) Morphology of Norway Spruce Tracheids with emphasis on cell wall organisation. Disseertation, Swedish University of Agricultural Sciences
3. Fengel D, Wegener G (1983) Wood—chemistry, ultrastructure, reactions. Walter de Gruyter, Berlin
4. Sippola M, Frühmann K (2002) Holzforschung 56:669
5. Tschegg S, Keunecke D, Tschegg E (2011) J Mech Behav Biomed Mater 4:688
6. Clair B, Arinero R, Lévèque G, Ramonda M, Thibaut B (2003) Int Assoc Wood Anat J 24(3):223
7. Goswami L, Dunlop J, Jungnikl K, Eder M et al (2008) Plant J 56:531
8. Burgert I, Frühmann K, Keckes J, Fratzl P, Tschegg S (2004) Trees 18:480
9. Kölln K, Grotkopp I, Burghammer M, Roth SV, Funari SS, Dommach M, Müller M (2005) J Synchrotron Radiat 12:739
10. Mott L, Groom L, Shaler S (2002) Wood Fiber Sci 34(2):221
11. Burgert I, Keckes J, Frühmann K, Fratzl P, Tschegg S (2002) Plant biol 4:9
12. Burgert I, Frühmann K, Keckes J, Fratzl P, Tschegg S (2003) Holzforschung 57:661
13. Burgert I, Eder M, Frühmann K, Keckes J, Fratzl P, Tschegg S (2005) Holzforschung 59:354
14. Keckes J, Burgert I, Frühmann K et al (2003) Nat Mater 2:810
15. Wimmer R, Lucas BN, Tsui TY, Oliver WC (1997) Wood Sci Technol 31:131
16. Gindl W, Gupta HS, Schöberl T, Lichtenegger HC, Fratzl P (2004) Appl Phys A 79:2069
17. Konnerth J, Gierlinger N, Keckes J, Gindl W (2009) J Mater Sci 44:4399. doi:10.1007/s10853-009-3665-7
18. Orso S, Wegst UGK, Arzt E (2006) J Mater Sci 41:5122. doi:10.1007/s10853-006-0072-1
19. Adusumalli RB, Raghavan R, Ghisleni R, Zimmermann T, Michler J (2010) Appl Phys A 100:447
20. Zhang X, Zhao Q, Wang S, Trejo R, Lara-Curzio E, Du G (2010) Compos A 41:632
21. Duchesne I, Daniel G (1999) Nord Pulp Pap Res J 14(2):129
22. Moser B, Wasmer K, Barbieri L, Michler J (2007) J Mater Res Soc 22(4):1004
23. Brändström J, Bardage SL, Daniel G, Nilsson T (2003) Int Assoc Wood Anat J 24(1):27
24. Abe H, Ohtani J, Fukazawa K (1991) Int Assoc Wood Anat Bull 12(4):431
25. Bergander A, Salmén L (2000) Holzforschung 54:654
26. Karlsson H (2006) Fiber guide—fiber analysis and process applications in the pulp and paper industry. AB Lorentzen & Wettre, Kista
27. Maurer A, Fengel D (1991) Holz als Roh und Werkstoff 13:323
28. He MY, Wissuchek DJ, Evans AG (1997) Acta Mater 45:2813